RSC Advances

PAPER

View Article Online
View Journal | View Issue

Cite this: *RSC Adv.*, 2020, **10**, 39000

Synthesis and stereocomplex formation of enantiomeric alternating copolymers with two types of chiral centers, poly(lactic acid-*alt*-2-hydroxybutanoic acid)s†

Hideto Tsuji, * Kazuya Nakayama and Yuki Arakawa

Stereocomplex (SC) formation was reported for the first time for enantiomeric alternating copolymers consisting of repeating units with two types of chiral centers, poly(lactic acid-*alt*-2-hydroxybutanoic acid)s [P(LA-*alt*-2HB)s]. L,L-Configured poly(L-lactic acid-*alt*-L-2-hydroxybutanoic acid) [P(LLA-*alt*-L-2HB)] and D,D-configured poly(D-lactic acid-*alt*-D-2-hydroxybutanoic acid) [P(DLA-*alt*-D-2HB)] were amorphous. Blends of P(LLA-*alt*-L-2HB) and P(DLA-*alt*-D-2HB) were crystallizable and showed typical SC-type wide-angle X-ray diffraction profiles similar to those reported for stereocomplexed blends of poly(L-lactic acid) and poly(D-lactic acid) homopolymers and of poly(L-2-hydroxybutanoic acid) and poly(D-2-hydroxybutanoic acid) homopolymers, and of L,L-configured poly(L-lactic acid-*co*-L-2-hydroxybutanoic acid) [P(LLA-*co*-L-2HB)] and D,D-configured poly(D-lactic acid-*co*-D-2-hydroxybutanoic acid) [P(DLA-*co*-D-2HB)] random copolymers. The melting temperature values and melting enthalpy values at 100% crystallinity for stereocomplexed solvent-evaporated and precipitated P(LLA-*alt*-L-2HB)/P(DLA-*alt*-D-2HB) blends were correspondingly 187.5 and 187.9 °C, and 98.1 and 91.8 J g^{-1}. Enantiomeric polymer blending of P(LLA-*alt*-L-2HB) and P(DLA-*alt*-D-2HB) can confer crystallizability by stereocomplexation and the biodegradable materials with a wide variety of physical properties and biodegradability are highly expected to be prepared by synthesis of alternating copolymers of various combinations of two types of chiral α-substituted 2-hydroxyalkanoic acid monomers and their SC crystallization.

Received 22nd July 2020
Accepted 1st October 2020

DOI: 10.1039/d0ra08351h

rsc.li/rsc-advances

1. Introduction

Poly(L-lactide) or poly(L-lactic acid) (PLLA), which is produced from renewable plant resources and biodegradable in the environment and the human body, has mechanical properties appropriate for a wide range of applications such as general, biomedical, pharmaceutical, and environmental applications.[1–11] To diversify its application, stereocomplex (SC) formation of PLLA with its enantiomer, poly(D-lactide) or poly(D-lactic acid) (PDLA) and D-configured poly(lactide) or poly(lactic acid) (PLA)-like homopolymers and random copolymers has been widely inquired.[12–23] Using the method of SC formation between PLLA and PDLA homopolymers and in stereo block copolymers, mechanical properties and resistance to thermal and hydrolytic degradation of PLA-based materials can be achieved.[12–23] Furthermore, SC formation of PLA-based block copolymers with water-soluble polymers facilitates the preparation of aqueous biomedical gels.[12–23] Various parameters affect SC formation. Such parameters include the types, concentrations and sequence of monomer units,[13,14,18,24–29] thermal history,[13,18,30,31] external forces,[13,18,32–36] the types and concentrations of solvents for casting,[18,37–39] the types and concentrations of third polymers and additives.[18,40–47]

Recently, the symmetry between PLLA and PDLA or their alternating packing was found to be retained in the SC crystal lattice,[48,49] whereas PDLA and PLLA chains were reported to be contained in the SC crystal lattice with a wide PLLA fractions from 30 to 70%.[50,51] The elastic modulus of the PLLA/PDLA SC crystalline region (20 GPa) in the direction parallel to the *c*-axis was higher than that of PLLA or PDLA homo-crystalline regions (14 GPa),[52] which should have been originated from the stronger interaction between PLLA and PDLA chains than that between

Department of Applied Chemistry and Life Science, Graduate School of Engineering, Toyohashi University of Technology, Tempaku-cho, Toyohashi, Aichi 441-8580, Japan. E-mail: ht003@edu.tut.ac.jp

† Electronic supplementary information (ESI) available: S1. Experimental section, S1.1. Materials and synthesis, S1.2. Sample preparation, S1.3. Physical measurements and observation, S2. ^{1}H NMR spectra of P(LLA-*alt*-L-2HB), P(DLA-*alt*-D-2HB), P(L-2HB), P(LLA-*co*-L-2HB), and PLLA (Fig. S1), S3. ^{13}C NMR spectra of P(LLA-*alt*-L-2HB) and P(DLA-*alt*-D-2HB) (Fig. S2), S4. ^{13}C NMR spectra of P(L-2HB), P(LLA-*co*-L-2HB), and PLLA (Fig. S3), S5. WAXD profile of *N*,*N*′-diisopropylurea (DIU) (Fig. S4), S6. Interplanar distance and crystalline diffraction angle values of samples (Table S1), S7. Crystallinity and thermal properties of samples (Table S2), S8. FTIR spectroscopy (Fig. S5 and Table S3). See DOI: 10.1039/d0ra08351h

PLLA chains or PDLA chains, as evidenced by atomic force microscopy.[53] Also, utilizing hydrogen-bonding, stereo diblock-like PLAs with high stereocomplexationability were prepared from PLLA and PDLA having 2-ureido-4[1*H*]-pyrimidinone terminal,[54] whereas stereo multiblock PLA was synthesized from DL-lactide at ambient temperature using achiral iron complexes.[55] The SC formation of lactic acid (LA) and α-amino acid-based enantiomeric random copoly(esteramides), poly(-lactic acid-*co*-alanine)s was reported.[56] Utilizing the stereocomplexed PLA nanofibers, highly transparent self-reinforced PLA composites were prepared.[57] PLA stereocomplexed materials having different memory shape effects were prepared by network formation or supramolecular formation and incorporation of elastomeric block.[58,59]

Similar to SC formation between PLLA and PDLA homopolymers, SC formation took place between the enantiomeric PLA-like homopolymers, poly(α-substituted 2-hydroxyalkanoic acid)s (Fig. 1), such as poly(2-hydroxybutanoic acid) [P(2HB)][18] and poly(2-hydroxy-3-methylbutanoic acid) [P(2H3MB)],[18] and poly(mandelic acid).[60] Hetero SC formation occurred between PLA and P(2HB), P(2HB) and P(2H3MB) with the different chemical structures and opposite configurations. Ternary SC formation took place in the blends of L- and D-configured P(2HB)s and L- or D-configured PLA,[18] L- and D-configured P(2H3MB)s and L- or D-configured P(2HB),[61] and D-configured PLA, L-configured P(2HB), and D-configured P(2H3MB) [or L-configured PLA, D-configured P(2HB), and L-configured P(2H3MB)],[62] whereas quaternary SC occurred in the blend of L- and D-configured P(2HB)s and L- and D-configured P(2H3MB)s.[18]

Also, SC formation took place in enantiomeric random copolymer blends of poly(L-lactic acid-*co*-L-2-hydroxybutanoic acid) [P(LLA-*co*-L-2HB)] (56/44) and poly(D-lactic acid-*co*-D-2-hydroxybutanoic acid) [P(DLA-*co*-D-2HB)] (52/48)[63] and of poly(L-lactic acid-*co*-L-2-hydroxy-3-methylbutanoic acid) [P(LLA-*co*-L-2H3MB)] (47/53) and poly(D-lactic acid-*co*-D-2-hydroxy-3-methylbutanoic acid) [P(DLA-*co*-D-2H3MB)] (47/53),[64] and the staggered random copolymers, L-configured P(LLA-*co*-L-2HB) (50/50) and D-configured poly(D-2-hydroxybutanoic acid-*co*-D-2-hydroxy-3-methylbutanoic acid) (50/50).[65] It should be noted that in these cases, all types of monomer units were confirmed to be packed in the SC crystalline lattice by wide-angle X-ray diffractometry (WAXD). This is in marked contrast with normal crystallization of random copolymers, wherein minor monomer units are excluded from and not included in the crystalline regions.

On the other hand, SC formation took place in enantiomeric alternating copolymer blends of poly(L-lactic acid-*alt*-6-hydroxycaproic acid) and poly(D-lactic acid-*alt*-6-hydroxycaproic acid)[66] and of poly(L-lactic acid-*alt*-glycolic acid) [P(LLA-*alt*-GA)] and poly(D-lactic acid-*alt*-glycolic acid) [P(DLA-*alt*-GA)].[67] These enantiomeric alternating copolymers which formed SC had the repeating or monomer units of lactic acid-6-hydroxycaproic acid or 6-hydroxycaproic acid–lactic acid and of lactic acid–glycolic acid or glycolic acid–lactic acid. In these repeating units, only one type of chiral center from lactic acid units existed. On the other hand, Tabata and Abe synthesized alternating copolymers composed of repeating or monomer units of two types of chiral centers, D,D-configured poly(D-lactic acid-*alt*-D-3-hydroxybutanoic acid) and L,D-configured poly(L-lactic acid-*alt*-D-3-hydroxybutanoic acid) and observed the melting temperature (T_m) difference between the two polymers (233 and 83 °C).[68]

In the present study, we synthesized enantiomeric alternating copolymers of poly(L-lactic acid-*alt*-L-2-hydroxybutanoic acid) [P(LLA-*alt*-L-2HB)] and poly(D-lactic acid-*alt*-D-2-hydroxybutanoic acid) [P(DLA-*alt*-D-2HB)] (Fig. 1) and report SC formation between alternating copolymer blends of P(LLA-*alt*-L-

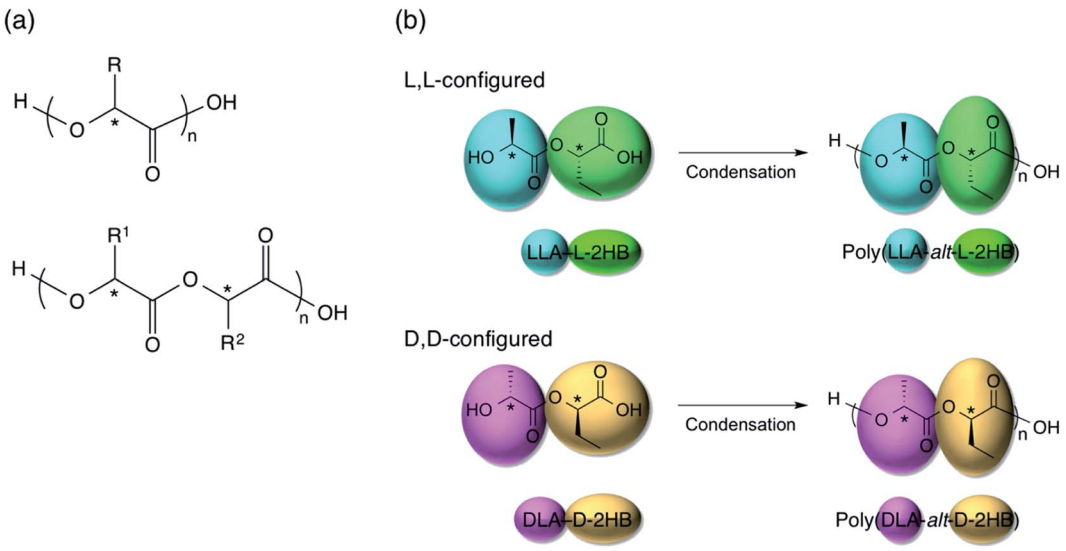

Fig. 1 Molecular structures of (a) PLA-like homopolymer [poly(α-substituted 2-hydroxyalkanoic acid)] consisting of repeating units with one type of chiral center and its alternating copolymer consisting of repeating units with two types of chiral centers and (b) synthetic strategy for P(LLA-*alt*-L-2HB) and P(DLA-*alt*-D-2HB) alternating copolymers. R: H [poly(glycolic acid), PGA], Me [poly(lactic acid), PLA], Et [poly(2-hydroxybutanoic acid), P(2HB)], i-Pr [poly(2-hydroxy-3-methylbutanoic acid), P(2H3MB)].

2HB) and P(DLA-*alt*-D-2HB). These alternating copolymers are composed of repeating unit of lactic acid-2-hydroxybutanoic acid or 2-hydroxybutanoic acid–lactic acid, which contain two types of chiral centers from lactic acid and 2-hydroxybutanoic acid units (Fig. 1). So, this is the first report for SC formation between enantiomeric alternating copolymers consisting of repeating units with two types of chiral centers. To investigate the physical properties, crystalline species, and crystallization behavior of unblended P(LLA-*alt*-L-2HB) and P(DLA-*alt*-D-2HB), and their blends, WAXD, differential scanning calorimetry (DSC), and Fourier transform infrared (FTIR) were carried out.

2. Experimental section

Materials and synthesis (Scheme 1),[69–72] sample preparation, physical measurements, and observation[62,64,67,73–75] were performed according to the literatures. The details of the experiments are stated in the ESI (Section S1).† The weight-average molecular weight (M_w), number average molecular weight (M_n), polydispersity index, and specific optical rotation in chloroform at 25 °C and 589 nm ($[\alpha]_{589}^{25}$) of P(LLA-*alt*-L-2HB) and P(DLA-*alt*-D-2HB) synthesized and used in the present study are 3.00×10^3, 3.08×10^3, g mol^{-1}, 1.53×10^3 and 1.54×10^3 g mol^{-1}, 1.96, 2.00, and −122.3, 120.3 deg dm^{-1} g^{-1} cm^3, respectively.

3. Results and discussion

3.1. Synthesis

In order to corroborate the alternating monomer unit sequences of the synthesized copolymers, ^{1}H and ^{13}C NMR measurements were performed (Fig. 2, S1(a), and S2†). All ^{1}H and ^{13}C NMR spectra for P(LLA-*alt*-L-2HB) and P(DLA-*alt*-D-2HB) are shown in ESI as Fig. S1(a) and S2,† respectively, together with those reported for P(L-2HB), P(LLA-*co*-L-2HB) random copolymer, and PLLA[75] [Fig. S1(b) and S3†]. The quartet and doublet peaks at 5.2 and 1.6 ppm observed for the ^{1}H NMR spectra of P(LLA-*alt*-L-2HB) and P(DLA-*alt*-D-2HB) are attributed to correspondingly methine (b) and methyl (a) protons of lactic acid (LA) units, whereas the quartet, multiplet, and triplet peaks at 5.0, 2.0, and 1.0 ppm are ascribed to correspondingly methine (e), methylene (d), and methyl (c) protons of 2-hydroxybutanoic acid (2HB) units [Fig. S1(a)†], in agreement with the ^{1}H NMR spectrum reported for the random copolymer, P(LLA-*co*-L-2HB).[75,76] However, methine peaks for LA and 2HB units [(b) and (e)] of P(LLA-*alt*-L-2HB) are sharp due to their regular alternating monomer sequences, in contrast with broad ones of P(LLA-*co*-L-2HB) random copolymer.

The singlet peaks seen at 169.0, 69.0, and 16.8 ppm for ^{13}C NMR spectra of P(LLA-*alt*-L-2HB) and P(DLA-*alt*-D-2HB) are attributed to carbonyl, methine, and methyl carbons of LA units, whereas those at 169.9, 73.6, 24.4, and 9.3 ppm are ascribed to carbonyl, methine, methylene, and methyl carbons of 2HB units [Fig. 2(b) and S2†].[75,77] In the case of P(LLA-*co*-L-2HB) random copolymer, triplet peaks are seen for the methylene carbon of 2HB units (24.2 ppm) and the methine carbon of LA units (16.8 ppm), whereas singlet peaks are observed for P(LLA-*alt*-L-2HB) and P(DLA-*alt*-D-2HB) [Fig. 2(b)]. Also, in the cases of P(LLA-*alt*-L-2HB) and P(DLA-*alt*-D-2HB), singlet peaks are observed for the carbonyl carbons of 2HB and LA units, whereas in the case of P(LLA-*co*-L-2HB) random copolymer, dual peaks are seen for carbonyl carbons of 2HB and LA units [Fig. S2(a) and S3(a)†]. The sharp ^{1}H NMR peaks and singlet ^{13}C NMR peaks of P(LLA-*alt*-L-2HB) and P(DLA-*alt*-D-2HB) indicate the fixed circumstances of LA and 2HB units in alternating

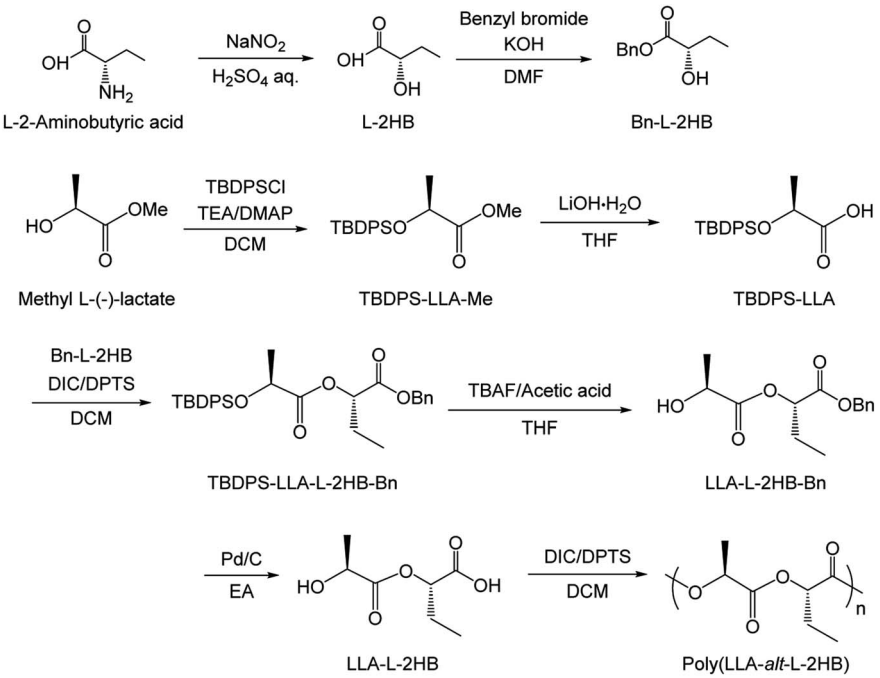

Scheme 1 Synthesis of poly(LLA-*alt*-L-2HB).

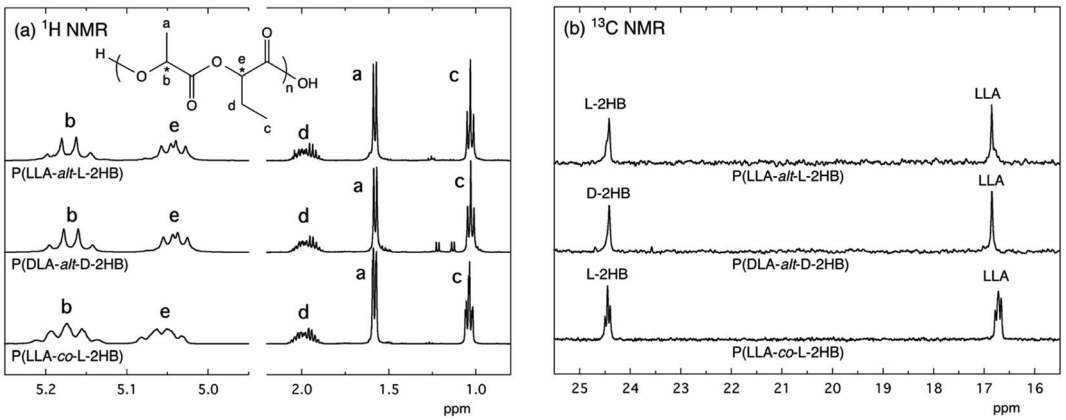

Fig. 2 (a) ^{1}H NMR spectra and (b) ^{13}C NMR spectra of methylene carbon of L-2HB units and methyl carbon of LLA units for P(LLA-*alt*-L-2HB) and P(DLA-*alt*-D-2HB) alternating copolymers and P(LLA-*co*-L-2HB) random copolymer in $CDCl_3$. The spectra for P(LLA-*co*-L-2HB) random copolymer were reproduced from ref. 75 with permission from Elsevier.

sequences but not in the various circumstances in random sequences, confirming the successful synthesis of P(LLA-*alt*-L-2HB) and P(DLA-*alt*-D-2HB) alternating copolymers.

3.2. Wide-angle X-ray diffractometry

For estimating the crystalline species and crystallinity (X_c) values of the samples, WAXD measurements were carried out [Fig. 3(a–c)]. The very weak crystalline peaks seen at 12.8, 19.6, 22.9, and 25.9° for solvent evaporated and precipitated P(DLA-*alt*-D-2HB) and precipitated P(LLA-*alt*-L-2HB)/P(DLA-*alt*-D-2HB) blend are ascribed to those of *N*,*N*′-diisopropylurea (DIU) formed during polymerization and remaining in the samples (Fig. S4†). The unblended P(LLA-*alt*-L-2HB) and P(DLA-*alt*-D-2HB) showed broad diffraction profiles, irrespective of sample preparation methods, indicating that the unblended polymer samples were amorphous. This result is in contrast with the results of P(LLA-*co*-L-2HB) (56/44) and P(DLA-*co*-D-2HB) (52/48) random copolymers[63,75] and P(LLA-*alt*-GA) and P(DLA-*alt*-GA) alternating copolymers,[67] which were homocrystallizable. The noncrystallizability of P(LLA-*alt*-L-2HB) and P(DLA-*alt*-D-2HB) may be due to their lower M_w values ($M_w = 3.0 \times 10^3$ and 3.1×10^3, g mol^{-1}, respectively) compared to those of the P(LLA-*co*-L-2HB) (56/44) and P(DLA-*co*-D-2HB) (52/48) random copolymers ($M_w = 1.4 \times 10^4$ and 1.6×10^4, g mol^{-1}, respectively) and P(LLA-*alt*-GA) and P(DLA-*alt*-GA) alternating copolymers ($M_w = 4.8 \times 10^3$ and 5.9×10^3, g mol^{-1}, respectively).

On the other hand, both solvent-evaporated and precipitated P(LLA-*alt*-L-2HB)/P(DLA-*alt*-D-2HB) blends showed the crystalline peaks at 11.4° (or 11.2°), 19.8° (or 19.5°), 22.9° (or 22.6°). Here, the data outside and inside parentheses are for the solvent-evaporated and precipitated samples, respectively. The diffraction patterns of P(LLA-*alt*-L-2HB)/P(DLA-*alt*-D-2HB) blends are similar to those of PLLA/PDLA homopolymer SC,[78] poly(L-2-hydroxybutanoic acid) [P(L-2HB)]/poly(D-2-hydroxybutanoic acid) [P(D-2HB)] homopolymer SC,[79] and P(LLA-*co*-L-2HB) (56/44)/P(DLA-*co*-D-2HB) (52/48) random copolymer SC,[63] but completely different from that of P(LLA-*alt*-GA)/P(DLA-*alt*-GA) alternating copolymer SC with the

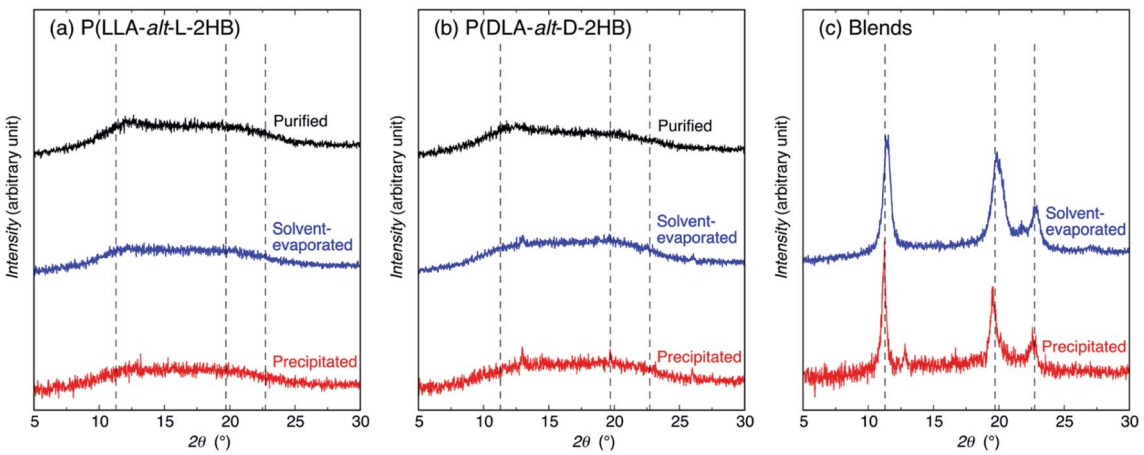

Fig. 3 WAXD profiles of purified, solvent-evaporated, and precipitated (a) P(LLA-*alt*-L-2HB), and (b) P(DLA-*alt*-D-2HB), and (c) solvent-evaporated and precipitated P(LLA-*alt*-L-2HB)/P(DLA-*alt*-D-2HB) blends. The main diffraction angles of P(LLA-*alt*-L-2HB)/P(DLA-*alt*-D-2HB) SC crystallites are shown with broken lines.

crystalline peaks at 17.3°, 18.5°, 21.3° (ref. 67) [Fig. 4]. The observed 2θ values of P(LLA-*alt*-L-2HB)/P(DLA-*alt*-D-2HB) blends are similar to those of P(LLA-*co*-L-2HB) (56/44)/P(DLA-*co*-D-2HB) (52/48) random copolymer SC [11.5° (or 11.3°), 20.0° (or 19.6° and 20.1°), 22.9° (or 22.7°), the data outside and inside parentheses are for the solvent-evaporated and melt-crystallized samples, respectively],[63] but lower and higher than those for the melt-crystallized PLLA/PDLA homopolymer SC (11.9°, 20.7°, 24.0°)[78] and P(L-2HB)/P(D-2HB) homopolymer SC (10.7°, 18.6° and 19.3°, 21.5°),[79] respectively. The interplanar distance (d) and crystalline diffraction angle (2θ) values of samples were obtained from Fig. 4, except for P(LLA-*alt*-GA)/P(DLA-*alt*-GA) alternating copolymer SC are tabulated in Table S1,† together with those for poly(L-2-hydroxy-3-methylbutanoic acid) [P(L-2H3MB)]/poly(D-2-hydroxy-3-methylbutanoic acid) [P(D-2H3MB)] homopolymer SC.[80] The diffraction peak patterns indicate SC formation between P(LLA-*alt*-L-2HB) and P(DLA-*alt*-D-2HB), whereas the 2θ and d values exhibit their SC crystalline lattice sizes are very similar to those of P(LLA-*co*-L-2HB) (56/44)/P(DLA-*co*-D-2HB) (52/48) random copolymer SC and between those of PLLA/PDLA homopolymer SC and P(L-2HB)/P(D-2HB) homopolymer SC. Very interestingly, comparison between the WAXD profiles of P(LLA-*alt*-L-2HB)/P(DLA-*alt*-D-2HB) SC and P(LLA-*alt*-GA)/P(DLA-*alt*-GA) SC [Fig. 4] reveals that their SC crystal lattice types of enantiomeric LA-based alternating copolymer are completely different.

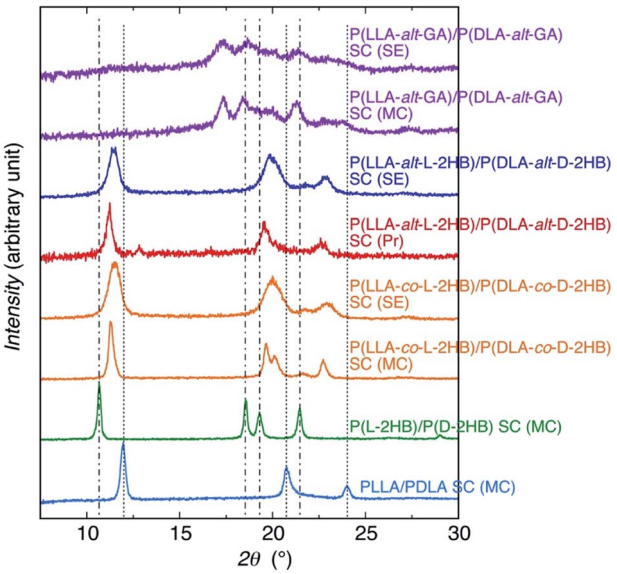

Fig. 4 WAXD profiles of solvent-evaporated (SE) and precipitated (Pr) P(LLA-*alt*-L-2HB)/P(DLA-*alt*-D-2HB) SC, together with solvent-evaporated and melt-crystallized (MC) P(LLA-*alt*-GA)/P(DLA-*alt*-GA) alternating copolymer SC,[67] solvent-evaporated and melt-crystallized P(LLA-*co*-L-2HB)/P(DLA-*co*-D-2HB) random copolymer SC,[63] melt-crystalized P(L-2HB)/P(D-2HB) homopolymer SC,[79] and melt-crystalized PLLA/PDLA homopolymer SC.[78] The main crystalline diffraction angles of SC crystallites for P(L-2HB)/P(D-2HB) homopolymer SC and PLLA/PDLA homopolymer SC are shown with dash-dotted lines and dotted lines, respectively. The data for P(LLA-*alt*-GA)/P(DLA-*alt*-GA) alternating copolymer SC, P(LLA-*co*-L-2HB)/P(DLA-*co*-D-2HB) random copolymer SC, P(L-2HB)/P(D-2HB) homopolymer SC, and PLLA/PDLA homopolymer SC were adapted from ref. 67, 63, 79, and 78 with permission from American Chemical Society, The Royal Society of Chemistry, American Chemical Society, and Wiley-VCH, respectively.

The crystallinity (X_c) values of the samples were obtained from the WAXD profiles in Fig. 3(a–c) and summarized in Table S2.† The X_c values of unblended P(LLA-*alt*-L-2HB) and P(DLA-*alt*-D-2HB) (both nil) are much lower than the purified and melt-crystallized unblended P(LLA-*co*-L-2HB) random copolymer (56/44) (43.7 and 36.5% for samples, respectively)[75] and purified and solvent-evaporated unblended P(LLA-*alt*-GA) and P(DLA-*alt*-GA) alternating copolymers [8.1% and nil for P(LLA-*alt*-GA) and 7.2 and 4.8% for P(DLA-*alt*-GA)]. On the other hand, the solvent-evaporated and precipitated P(LLA-*alt*-L-2HB)/P(DLA-*alt*-D-2HB) blends are 66.7 and 60.8%, respectively, which are lower than those reported for the solvent-evaporated and melt-crystallized P(LLA-*co*-L-2HB) (56/44)/P(DLA-*co*-D-2HB) (52/48) random copolymer blends (82.5 and 77.7%, respectively),[63] but much higher than those reported for solvent-evaporated and melt-crystallized P(LLA-*alt*-GA)/P(DLA-*alt*-GA) alternating copolymer blends (20.8 and 29.2%, respectively). The lower X_c values of unblended P(LLA-*alt*-L-2HB) and P(DLA-*alt*-D-2HB) compared to those of unblended P(LLA-*co*-L-2HB) random copolymer (56/44) and unblended P(LLA-*alt*-GA) and P(DLA-*alt*-GA) alternating copolymers and the lower X_c values of P(LLA-*alt*-L-2HB)/P(DLA-*alt*-D-2HB) blends compared to those of P(LLA-*co*-L-2HB) (56/44)/P(DLA-*co*-D-2HB) (52/48) random copolymer blends can be ascribed to the lower molecular weights of P(LLA-*alt*-L-2HB) and P(DLA-*alt*-D-2HB). Interestingly, despite the lower X_c values of unblended P(LLA-*alt*-L-2HB) and P(DLA-*alt*-D-2HB) compared to those of unblended P(LLA-*alt*-GA) and P(DLA-*alt*-GA) alternating copolymers, the higher X_c values of P(LLA-*alt*-L-2HB)/P(DLA-*alt*-D-2HB) blends compared to those of P(LLA-*alt*-GA)/P(DLA-*alt*-GA) alternating copolymer blends exhibit that dual chiral centers per a repeating unit in P(LLA-*alt*-L-2HB) and P(DLA-*alt*-D-2HB) enhanced the crystallizability of the enantiomeric polymers by stereocomplexation compared to one chiral center per a repeating unit in P(LLA-*alt*-GA) and P(DLA-*alt*-GA).

3.3. Differential scanning calorimetry

For estimating crystallization and thermal properties of the samples, DSC measurements were conducted (Fig. 5). The glass transition temperature (T_g), T_m, and melting enthalpy (ΔH_m) were estimated from the DSC thermograms in Fig. 5 and are summarized in Table S2.† The unblended P(LLA-*alt*-L-2HB) and P(DLA-*alt*-D-2HB) show only glass transition peak at around 15.5–40.4 °C without melting peak, regardless of preparation methods, confirming the WAXD result that unblended P(LLA-*alt*-L-2HB) and P(DLA-*alt*-D-2HB) were amorphous. On the other hand, the solvent-evaporated and precipitated P(LLA-*alt*-L-2HB)/P(DLA-*alt*-D-2HB) blends showed glass transition and melting peaks correspondingly at 33.7, 36.3 °C and 187.5, 187.9 °C. The T_m values for P(LLA-*alt*-L-2HB)/P(DLA-*alt*-D-2HB) (M_w = 3.0 × 10^3 and 3.1 × 10^3, g mol^{-1}, respectively) blends are higher than those for solvent-evaporated and melt-crystallized (T_c = 70 °C) P(L-2HB)/P(D-2HB) (M_w = 1.8 × 10^3 and 3.3 × 10^3, g mol^{-1}, respectively) homopolymer blends (T_m = 173.0 and 172.1 °C,

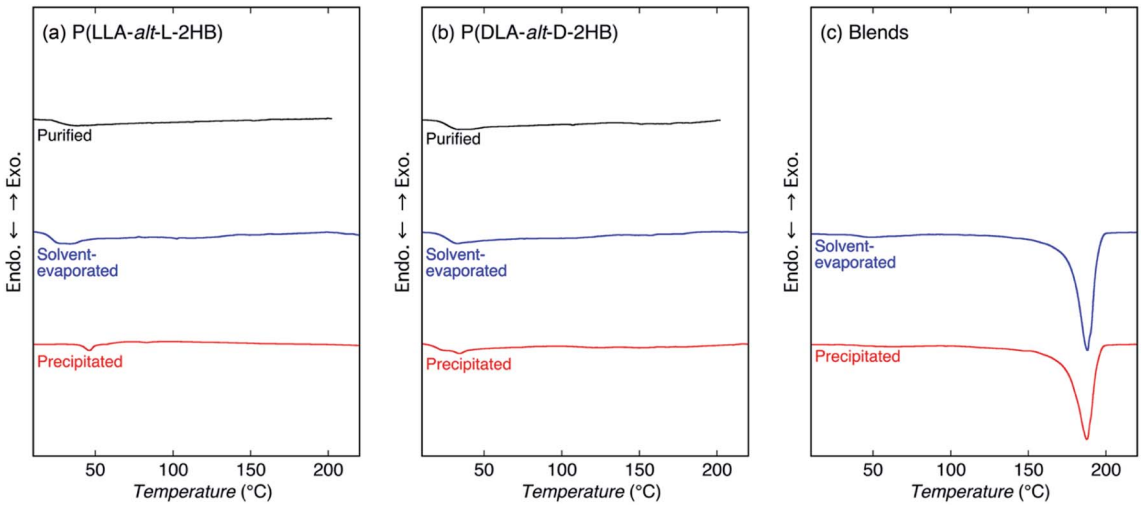

Fig. 5 DSC thermograms of purified, solvent-evaporated, and precipitated (a) P(LLA-*alt*-L-2HB) and (b) P(DLA-*alt*-D-2HB), and (c) solvent-evaporated and precipitated P(LLA-*alt*-L-2HB)/P(DLA-*alt*-D-2HB) blends on first heating scan at a rate of 10 °C min^{-1}.

respectively)[81] but lower than those for melt-crystallized (T_c = 130 °C) PLLA/PDLA (M_w = 4.0 × 10^3 and 5.4 × 10^3, g mol^{-1}, respectively) homopolymer blends (T_m = 197.5 °C),[78] and solvent-evaporated and melt-crystallized (T_c = 160 °C) P(LLA-*co*-L-2HB) (56/44)/P(DLA-*co*-D-2HB) (52/48) (M_w = 1.4 × 10^4 and 1.6 × 10^4, g mol^{-1}, respectively) random copolymer blends (203.6 and 198.4 °C),[63] and solvent evaporated and melt-crystallized (T_c = 100 °C) P(LLA-*alt*-GA)/P(DLA-*alt*-GA) (M_w = 4.8 × 10^3 and 5.9 × 10^3, g mol^{-1}, respectively) blends (187.8 and 187.6 °C).[67] The lower T_m values of P(LLA-*alt*-L-2HB) and P(DLA-*alt*-D-2HB) can be attributable to the low molecular weights compared to those of PLLA and PDLA, P(LLA-*co*-L-2HB) (56/44) and P(DLA-*co*-D-2HB) (52/48), and P(LLA-*alt*-GA) and P(DLA-*alt*-GA).

Using the ΔH_m and X_c of solvent-evaporated (65.4 J g^{-1} and 66.7%) and precipitated (55.8 J g^{-1} and 60.8%) P(LLA-*alt*-L-2HB)/P(DLA-*alt*-D-2HB) blends, ΔH_m values at X_c = 100%, *i.e.*, ΔH_m^0 values were estimated to be 98.1 and 91.8 J g^{-1}, respectively. Using the ΔH_m and X_c of solvent-evaporated (83.7 J g^{-1} and 82.5%) and precipitated (74.3 J g^{-1} and 77.7%) P(LLA-*co*-L-2HB)/P(DLA-*co*-D-2HB) random copolymer blends,[63] ΔH_m^0 values were evaluated to be 101.5 and 95.6 J g^{-1}, respectively. Also, using the ΔH_m and X_c of solvent-evaporated (53.4 J g^{-1} and 20.8%) and melt-crystallized (67.7 J g^{-1} and 29.2%) P(LLA-*alt*-GA)/P(DLA-*alt*-GA) blends, ΔH_m^0 values were estimated to be 256.7 and 231.8 J g^{-1},[67] respectively, which are much higher than ΔH_m^0 value of poly(glycolic acid) (206 J g^{-1})[82] and PLLA/PDLA homopolymer SC (142 (ref. 83) and 146 (ref. 77) J g^{-1}). Surprisingly, the ΔH_m^0 values of P(LLA-*alt*-L-2HB)/P(DLA-*alt*-D-2HB) blends are similar to those of P(LLA-*co*-L-2HB)/P(DLA-*co*-D-2HB) random copolymer blends, despite the fact that P(LLA-*alt*-L-2HB) and P(DLA-*alt*-D-2HB) have higher sequential regularity compared to that of P(LLA-*co*-L-2HB) and P(DLA-*co*-D-2HB). This finding can also be explained by the fact that the molecular weights of P(LLA-*alt*-L-2HB) and P(DLA-*alt*-D-2HB) are lower than those of P(LLA-*co*-L-2HB) and P(DLA-*co*-D-2HB) random copolymers. The lower molecular weights or increased density of chain terminals of the former should have increased the defects in the crystalline regions, resulting in lower ΔH_m and ΔH_m^0 values.

Finally, the present study reveals that even though alternating copolymers with two types of chiral centers per a repeating unit is amorphous, their enantiomeric polymer blending can impose crystallizability by stereocomplexation and it is strongly expected that the biodegradable materials with a wide range of physical properties and biodegradability can be prepared by various combinations of two types of chiral α-substituted 2-hydroxyalkanoic acid monomers. For this purpose, accumulating the information of physical properties and biodegradability of SCs from enantiomeric alternating α-substituted hydroxyalkanoic acid-based polymers with various combinations of chiral monomers is required.

4. Conclusions

SC formation was reported for the first time for enantiomeric alternating copolymers with two types of chiral centers per a repeating unit, P(LA-*alt*-2HB). L,L-Configured P(LLA-*alt*-L-2HB) and D,D-configured P(DLA-*alt*-D-2HB) were amorphous polymers. P(LLA-*alt*-L-2HB)/P(DLA-*alt*-D-2HB) blends were crystallizable and showed typical SC-type wide-angle X-ray diffraction profiles similar to those reported for PLLA/PDLA homopolymer SC, P(L-2HB)/P(D-2HB) homopolymer SC, and P(LLA-*co*-L-2HB)/P(DLA-*co*-D-2HB) random copolymer SC. The T_m and ΔH_m^0 values for stereocomplexed solvent-evaporated and precipitated P(LLA-*alt*-L-2HB)/P(DLA-*alt*-D-2HB) blends were correspondingly 187.5 and 187.9 °C, and 98.1 and 91.8 J g^{-1}. Enantiomeric polymer blending of P(LLA-*alt*-L-2HB) and P(DLA-*alt*-D-2HB) can grant crystallizability by stereocomplexation and the biodegradable materials with a wide variety of physical properties and biodegradability are highly expected to be prepared by synthesis of alternating copolymers of various combinations of two types of chiral α-substituted 2-hydroxyalkanoic acid monomers and their SC crystallization.

Abbreviations

2HB	2-Hydroxybutanoic acid
ΔH_m	Melting enthalpy
ΔH_m^0	ΔH_m at $X_c = 100\%$
DIU	*N*,*N*′-Diisopropylurea
DSC	Differential scanning calorimetry
M_n	Number average molecular weight
MC	Melt-crystallized
M_w	Weight-average molecular weight
LA	Lactic acid
P(2H3MB)	Poly(2-hydroxy-3-methylbutanoic acid)
P(2HB)	Poly(2-hydroxybutanoic acid)
P(D-2HB)	Poly(D-2-hydroxybutanoic acid)
P(D-2H3MB)	Poly(D-2-hydroxy-3-methylbutanoic acid)
PDLA	Poly(D-lactide) or poly(D-lactic acid)
P(DLA-*alt*-D-2HB)	Poly(D-lactic acid-*alt*-D-2-hydroxybutanoic acid)
P(DLA-*alt*-GA)	Poly(D-lactic acid-*alt*-glycolic acid)
P(DLA-*co*-D-2H3MB)	Poly(D-lactic acid-*co*-D-2-hydroxy-3-methylbutanoic acid)
P(DLA-*co*-D-2HB)	Poly(D-lactic acid-*co*-D-2-hydroxybutanoic acid)
P(L-2HB)	Poly(L-2-hydroxybutanoic acid)
P(L-2H3MB)	Poly(L-2-hydroxy-3-methylbutanoic acid)
PLA	Poly(lactide) or poly(lactic acid)
P(LA-*alt*-2HB)	Poly(lactic acid-*alt*-2-hydroxybutanoic acid)
PLLA	Poly(L-lactide) or poly(L-lactic acid)
P(LLA-*alt*-GA)	Poly(L-lactic acid-*alt*-glycolic acid)
P(LLA-*alt*-L-2HB)	Poly(L-lactic acid-*alt*-L-2-hydroxybutanoic acid)
P(LLA-*co*-L-2H3MB)	Poly(L-lactic acid-*co*-L-2-hydroxy-3-methylbutanoic acid)
P(LLA-*co*-L-2HB)	Poly(L-lactic acid-*co*-L-2-hydroxybutanoic acid)
Pr	Precipitated
SC	Stereocomplex
SE	Solvent-evaporated
$[\alpha]$	Specific optical rotation
T_g	Glass transition temperature
T_m	Melting temperature
X_c	Crystallinity
WAXD	Wide-angle X-ray diffractometry

Conflicts of interest

There are no conflicts to declare.

Acknowledgements

This research was supported by the research grants from The Hibi Science Foundation and JSPS (KAKENHI, Grant Number 16K05912).

References

1 M. Vert, J. Feijen, A.-C. Albertsson, G. Scott and E. Chiellini, *Biodegradable Polymers and Plastics*, Royal Society of Chemistry, Cambridge, 1992.
2 D. P. Mobley, *Plastics from Microbes*, Hanser Publishers, New York, 1994.
3 M. Vert, G. Schwarch and J. Coudane, *J. Macromol. Sci., Part A: Pure Appl. Chem.*, 1995, **32**, 787–796.
4 A. J. Domb, J. Kost and D. M. Wieseman, *Handbook of Biodegradable Polymers (Drug Targeting and Delivery)*, Harwood Academic Publishers, Amsterdam (The Netherlands), 1997, vol. 7.
5 D. L. Kaplan, *Biopolymers from Renewable Resources*, Springer, Berlin (Germany), 1998.
6 D. A. Garlotta, *J. Polym. Environ.*, 2001, **9**, 63–84.
7 A. Södergård and M. Stolt, *Prog. Polym. Sci.*, 2002, **27**, 1123–1163.
8 A.-C. Albertsson, *Degradable Aliphatic Polyesters (Advances in Polymer Science)*, Springer, Berlin (Germany), 2002, vol. 157.
9 Y. Doi and A. Steinbüchel, *Polyesters I, II, III (Biopolymers, Vol. 3a, 3b, 4)*, Wiley-VCH, Weinheim (Germany), 2002.
10 R. Auras, L.-T. Lim, S. E. M. Selke and H. Tsuji, *Poly(lactic acid): synthesis, structures, properties, processing, and applications*, (Wiley Series on Polymer Engineering and Technology), John Wiley & Sons, Inc., NJ, 2010.
11 H. Tsuji, in *Poly(Lactic Acid). Bio-Based Plastics: Materials and Applications*, ed. S. Kabasi, Wiley & Sons, Ltd, Chichester (UK), 2014, ch. 8, pp. 171–239.
12 J. Slager and A. J. Domb, *Adv. Drug Delivery Rev.*, 2003, **55**, 549–583.
13 H. Tsuji, *Macromol. Biosci.*, 2005, **5**, 569–597.
14 K. Fukushima and Y. Kimura, *Polym. Int.*, 2006, **55**, 626–642.
15 P. Pan and Y. Inoue, *Prog. Polym. Sci.*, 2009, **34**, 605–640.
16 M. Saravanan and A. J. Domb, *Eur. J. Nanomed.*, 2013, **5**, 81–86.
17 Y. Jing, C. Quan, Q. Jiang, C. Zhang and Z. Chao, *Polym. Rev.*, 2016, **56**, 262–286.
18 H. Tsuji, *Adv. Drug Delivery Rev.*, 2016, **107**, 97–135.
19 B. H. Tan, J. K. Muiruri, Z. Li and C. He, *ACS Sustainable Chem. Eng.*, 2016, **4**, 5370–5391.
20 Z. Li, B. H. Tan, T. Lin and C. He, *Prog. Polym. Sci.*, 2016, **62**, 22–72.
21 H. Bai, S. Deng, D. Bai, Q. Zhang and Q. Fu, *Macromol. Rapid Commun.*, 2017, **38**, 1700454.
22 Q. Xie, C. Yu and P. Pan, in *Crystallization in Multiphase Polymer Systems*, ed. S. Thomas, M. Arif P., E. Bhoje Gowd and N. Kalarikkal, Elsevier Inc., Amsterdam (Netherlands), 2018, ch. 17, pp. 535–573.
23 D. Bandelli, J. Alex, C. Weber and U. S. Schubert, *Macromol. Rapid Commun.*, 2020, **41**, 1900560.
24 N. Yui, P. J. Dijkstra and J. Feijen, *Macromol. Chem. Phys.*, 1990, **191**, 481–488.
25 K. Fukushima, Y. Furuhashi, K. Sogo, S. Miura and Y. Kimura, *Macromol. Biosci.*, 2005, **5**, 21–29.
26 M. H. Rahaman and H. Tsuji, *Macromol. React. Eng.*, 2012, **6**, 446–457.
27 K. Masutani, C. W. Lee and Y. Kimura, *Polym. J.*, 2013, **45**, 427–435.
28 L. Han, G. Shan, Y. Bao and P. Pan, *J. Phys. Chem. B*, 2015, **119**, 14270–14279.

29 L. Han, Q. Xie, J. Bao, G. Shan, Y. Bao and P. Pan, *Polym. Chem.*, 2017, **8**, 1006–1016.
30 J. Zhang, K. Tashiro, H. Tsuji and A. J. Domb, *Macromolecules*, 2007, **40**, 1049–1054.
31 H. Tsuji and Y. Ikada, *Macromol. Chem. Phys.*, 1996, **197**, 3483–3499.
32 H. Tsuji, S.-H. Hyon and Y. Ikada, *Macromolecules*, 1991, **24**, 5657–5662.
33 H. Tsuji, M. Nakano, M. Hashimoto, K. Takashima, S. Katsura and A. Mizuno, *Biomacromolecules*, 2006, **7**, 3316–3320.
34 K. Hemmi, G. Matsuba, H. Tsuji, T. Kawai, T. Kanaya, K. Toyohara, A. Oda and K. Endou, *J. Appl. Crystallogr.*, 2014, **47**, 14–21.
35 Y. Duan, J. Liu, H. Sato, J. Zhang, H. Tsuji, Y. Ozaki and S. Yan, *Biomacromolecules*, 2006, **7**, 2728–2735.
36 T. Serizawa, H. Yamashita, T. Fujiwara, Y. Kimura and M. Akashi, *Macromolecules*, 2001, **34**, 1996–2001.
37 H. Tsuji and S. Yamamoto, *Macromol. Mater. Eng.*, 2011, **296**, 583–589.
38 Y. Furuhashi and N. Yoshie, *Polym. Int.*, 2012, **61**, 301–306.
39 K. Fukushima, Y.-H. Chang and Y. Kimura, *Macromol. Biosci.*, 2007, **7**, 829–835.
40 P. Purnama and S. H. Kim, *Macromolecules*, 2010, **43**, 1137–1142.
41 C. Samuel, J. Cayuela, I. Barakat, A. J. Müller, J.-M. Raquez and P. Dubois, *ACS Appl. Mater. Interfaces*, 2013, **5**, 11797–11807.
42 R.-Y. Bao, W. Yang, X.-F. Wei, B.-H. Xie and M.-B. Yang, *ACS Sustainable Chem. Eng.*, 2014, **2**, 2301–2309.
43 J. Zhu, B. Na, R. Lv and C. Li, *Polym. Int.*, 2014, **63**, 1101–1104.
44 L. Gardella, D. Furfaro, M. Galimberti and O. Monticelli, *Green Chem.*, 2015, **17**, 4082–4088.
45 H. Xu, D. Wu, X. Yang, L. Xie and M. Hakkarainen, *Macromolecules*, 2015, **48**, 2127–2137.
46 L. Han, P. Pan, G. Shan and Y. Bao, *Polymer*, 2015, **63**, 144–153.
47 J. Bao, X. Xue, K. Li, X. Chang and Q. Xie, *J. Phys. Chem. B*, 2017, **121**, 6934–6943.
48 F. Zhang, H.-W. Wang, K. Tominaga, M. Hayashi, S. Lee and T. Nishino, *J. Phys. Chem. Lett.*, 2016, **7**, 4671–4676.
49 W. Zhou, K. Wang, S. Wang, S. Yuan, W. Chen, T. Konishi and T. Miyoshi, *ACS Macro Lett.*, 2018, **7**, 667–671.
50 K. Tashiro, H. Wang, N. Kouno, J. Koshobu and K. Watanabe, *Macromolecules*, 2017, **50**, 8066–8071.
51 K. Tashiro, N. Kouno, H. Wang and H. Tsuji, *Macromolecules*, 2017, **50**, 8048–8065.
52 S. Lee, M. Kimoto, M. Tanaka, H. Tsuji and T. Nishino, *Polymer*, 2018, **138**, 124–131.
53 S. Fujishiro, D. Minamino, I. Obataya, N. Saitoh, Y. Hosokawa and H. Ajiro, *Chem. Lett.*, 2018, **47**, 82–84.
54 J. Bao, X. Chang, G. Shan, Y. Bao and P. Pan, *Polym. Chem.*, 2016, **7**, 4891–4900.
55 P. Marin, M. J.-L. Tschan, F. Isnard, C. Robert, P. Haquette, X. Trivelli, L.-M. Chamoreau, V. Guérineau, I. del Rosal, M. Laurent, V. Venditto and C. M. Thomas, *Angew. Chem., Int. Ed.*, 2019, **58**, 12585–12589.
56 H. Tsuji, S. Sato, N. Masaki, Y. Arakawa, A. Kuzuya and Y. Ohya, *Polym. Chem.*, 2018, **9**, 565–575.
57 N. Kurokawa and A. Hotta, *Polymer*, 2018, **153**, 214–222.
58 J. Zhou, H. Cao, R. Chang, G. Shan, Y. Bao and P. Pan, *ACS Macro Lett.*, 2018, **7**, 233–7238.
59 R. Chang, G. Shan, Y. Bao and P. Pan, *Macromolecules*, 2015, **48**, 7872–7881.
60 M. Li, Y. Tao, J. Tang, Y. Wang, X. Zhang, Y. Tao and X. Wang, *J. Am. Chem. Soc.*, 2019, **141**, 281–289.
61 H. Tsuji, N. Masaki, Y. Arakawa, K. Iguchi and T. Sobue, *Cryst. Growth Des.*, 2018, **18**, 521–530.
62 H. Tsuji, S. Noda, T. Kimura, T. Sobue and Y. Arakawa, *Sci. Rep.*, 2017, **7**, 45170.
63 H. Tsuji and T. Sobue, *RSC Adv.*, 2015, **5**, 83331–83342.
64 H. Tsuji, K. Osanai and Y. Arakawa, *Cryst. Growth Des.*, 2020, **20**, 1047–1057.
65 H. Tsuji, K. Osanai and Y. Arakawa, *Cryst. Growth Des.*, 2018, **18**, 6009–6019.
66 F.-R. Zeng, J.-M. Ma, L.-H. Sun, Z. Zeng, H. Jiang and Z.-L. Li, *Macromol. Chem. Phys.*, 2018, **219**, 1800031.
67 H. Tsuji, M. Yamasaki and Y. Arakawa, *ACS Appl. Polym. Mater.*, 2019, **1**, 1476–1484.
68 Y. Tabata and H. Abe, *Macromolecules*, 2014, **47**, 7354–7361.
69 J. S. Moore and S. I. Stupp, *Macromolecules*, 1990, **23**, 65–70.
70 R. M. Stayshich and T. Y. Meyer, *J. Polym. Sci., Part A: Polym. Chem.*, 2008, **46**, 4704–4711.
71 R. M. Stayshich and T. Y. Meyer, *J. Am. Chem. Soc.*, 2010, **132**, 10920–10934.
72 H. Tsuji and Y. Arakawa, *Polym. Chem.*, 2018, **9**, 2446–2457.
73 Y. Sakamoto and H. Tsuji, *Polymer*, 2013, **54**, 2422–2434.
74 H. Tsuji, Y. Arakawa and N. Matsumura, *Polym. Bull.*, 2019, **76**, 1199–1216.
75 H. Tsuji and T. Sobue, *Polymer*, 2015, **72**, 202–211.
76 K. Matsumoto, S. Terai, A. Ishiyama, J. Sun, T. Kabe, Y. Song, J. M. Nduko, T. Iwata and S. Taguchi, *Biomacromolecules*, 2013, **14**, 1913–1918.
77 H. Tsuji, F. Horri, S.-H. Hyon and Y. Ikada, *Macromolecules*, 1992, **25**, 4114–4118.
78 L. Bouapao and H. Tsuji, *Macromol. Chem. Phys.*, 2009, **210**, 993–1003.
79 H. Tsuji and A. Okumura, *Macromolecules*, 2009, **42**, 7263–7266.
80 H. Tsuji and T. Sobue, *Polymer*, 2015, **69**, 186–192.
81 H. Tsuji and S. Shimizu, *Polymer*, 2012, **53**, 5385–5392.
82 L. I. Ramdhanie, S. R. Aubuchon, E. D. Boland, D. C. Knapp, C. P. Barnes, D. G. Simpson, G. E. Wnek and G. L. Bowlin, *Polym. J.*, 2006, **38**, 1137–1145.
83 G. L. Loomis, J. R. Murdoch and K. H. Gardner, *Polym. Prepr. (Am. Chem. Soc., Div. Polym. Chem.)*, 1990, **31**, 55.